Review copy – not for distribution

(pss-logo will be inserted here by the publisher)

Direct observation of flow in semi-solid alloys by synchrotron-based x-ray micro-radioscopy

Simon Zabler[*,1], Alexander Rack[2], Antonio Rueda[3], Lukas Helfen[2], Francisco García-Moreno[3] and John Banhart[3]

[1] Institut für Werkstofftechnik, Technische Universität Berlin, Strasse des 17. Juni 135, D- 10623 Berlin, Germany
[2] Institut für Synchrotronstrahlung (ISS/ANKA), Forschungszentrum Karlsruhe, PO Box 3640, D-76021 Karlsruhe, Germany
[3] Institute of Materials, Helmholtz Centre Berlin for Materials and Energy, Glienicker Strasse 100, D- 14109 Berlin, Germany

Received ZZZ, revised ZZZ, accepted ZZZ
Published online ZZZ (Dates will be provided by the publisher.)

PACS 00.00.Xx, 11.11.Yy, 22.22.Zz, 33.33.Aa (Please insert 4 to 6 PACS codes from the enclosed list or from www.aip.org/pacs)

* Corresponding author: e-mail simon.zabler@tu-berlin.de, Phone: +49 (0)30 314 22990, Fax: +49 (0)30 314 26673

The flow of a semi-solid aluminium-germanium alloy Al-Ge32 (wt.%) into a thin cavity was monitored by in-situ micro-radioscopy using white hard x-ray synchrotron radiation. X-ray images were recorded at an acquisition speed of 67 frames/ sec using an indirect X-ray pixel detector in combination with a CMOS camera. Liquid drainage and de- / re-agglomeration of small aluminium-rich solid particle clusters – associated with the slurry's thixotropic behaviour – could be visualized. The technique and first results obtained are discussed in terms of their future application and possible improvements.

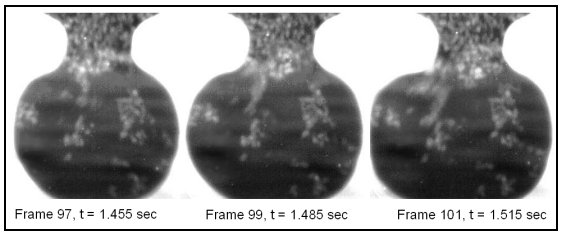

Radiographic image sequence showing fast injection of semi-solid slurry into the mould. Solid Al-rich particles appear brighter than the surrounding liquid Al-Ge melt.

Copyright line will be provided by the publisher

1 Introduction For the production of both high-quality and light-weight metallic components semi-solid casting (SSC) is a promising process [1]. SSC features a very good die-filling and a fine equiaxed microstructure. Examples for SSC are thixo- and rheocasting processes. Here, pre-alloyed material is commonly brought to a temperature above the solidus and below the liquidus temperature either from the solid or from the liquid, respectively. This results in the coexistence of solid and liquid phase and the forming of a slurry. Such slurries are known for their shear-thinning behaviour. For binary alloys such as Al-Ge or Al-Si, the solid phase is enriched with the majority element (here: aluminium) and is morphologically a collection of sponge-like particle agglomerates that continuously undergo morphological transformations, e.g. coarsening [2]. The liquid phase is a mixture of the remaining element having equilibrium concentration and filling the inter-particle as well as the inter-granular spaces. For larger solid volume fractions (>30%) the solid grains tend to agglomerate, forming a bulk skeleton which makes it difficult to distinguish between different grains in normal microscopes (etching has to be applied) or high-resolution X-ray images (grains and boundaries can only be visualised using X-rays in combination with diffraction-based contrast modes [3,4]). For optimal SSC, a fine equiaxed microstructure is desired, since non-equiaxed and coarse grains, especially dendrites, are known to raise the viscosity of the semi-solid slurry causing incomplete die filling [5]. When the fine-grained material is injected into a casting die at high pressure, a spontaneous drop in the flow resistance of the slurry is observed. This is due to shear forces which cause de-agglomeration of the solid grains, and possibly also fracture of some grains into smaller particles and/or clusters [6]. Spencer et al. were the first ones

Copyright line will be provided by the publisher

to observe the apparent viscosity of semi-solid Sn-Pb alloy to decrease under shearing by some orders of magnitude [7]. Commonly variations from 10^{7} down to 10^{-1} Pa·s are observed for shearing rates ranging from 10^{-5} to 10^{3} s^{-1} [8,9]. Many empirical and theoretical models have been developed - for a review see [1,6] - some of which consider particle shape and connectivity as fundamental parameters determining the shear thinning properties of the mixture. Because the viscosity depends strongly on the initial microstructure of the feedstock material it is difficult to include the shear-thinning behaviour into flow simulations

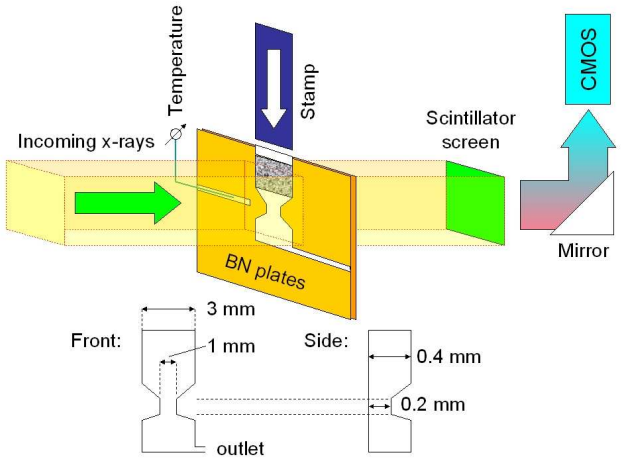

Figure 1 Schematic drawing of the *in situ* micro-radioscopy setup.

of the real casting processes [10]. In order to parameterize such flow simulations, a relationship between industrial SSC and results from viscosity measurements in the rheometer is commonly established: comparing microscopic images of plane sections that are cut from quenched samples which are assumed to represent the industrial process [11]. Flow simulations are then used to optimize the die geometry for a homogeneous filling. Since the experimental conditions do not allow for a direct observation of the solid particle flow in the die, only little is known about the dynamic behaviour of the semi-solid mixture when it is injected into a thin cavity at high pressure. In this paper, we present a fast x-ray radioscopy study to directly visualize the semi-solid microstructure in-situ during the injection process. Such techniques have already been used to study convective flow in opaque liquid metals [12, 13]. Boden et. al recently used a commercial x-ray tube to study convection during solidification of Ga-In alloy at a rate of approximately 2 frames/ sec. Since such acquisition rates are too slow to study the movement of solid particles in liquid melt during casting we used synchrotron imaging with a data acquisition rate of 67 frames/ sec employing a polychromatic x-ray beam.

2 Materials and method

2.1 Experimental An experimental setup for in situ flow monitoring of semi-solid slurry was constructed by the Helmholtz Centre Berlin and the Federal Institute for Materials Research and Testing (BAM), both Germany, and was assembled at the ID19 beamline of the European Synchrotron Radiation Facility (ESRF) in Grenoble, France. The setup is shown in detail in Fig. 1. It is similar to the one that was recently used for measuring particle coarsening in semi-solid Al-Ge32 alloy [2]. At the beginning of the experiment a small piece (3 mm x 3 mm x 0.4 mm) of grain refined Al-Ge32 alloy (including 4% AlTiB5 grain refiner – AFM Affilips, Netherlands) was inserted into a flat injection reservoir between two 1 mm thick boron nitride (BN) plates. BN was used because of its high melting point and low x-ray absorption. Furthermore, BN does not react with the Al-Ge melt. Below the reservoir a bottleneck-shaped flow channel was machined into the plates, reducing the effective cross-section to 1 mm x 0.2 mm. Further below this ~1 mm long bottleneck, there was a recipient of the same dimensions as the reservoir at the top, with a small gas outlet to the side. The BN plates are clamped between two U-shaped ceramic supports and the whole setup is positioned such that the metallic sheet is facing the incoming X-ray beam. For heating the sample, we used two Osram Xenophot 64635 HLX (150 W) heating lamps, one on each side of the sample with the BN plates slightly moved out of the lamps' focus to achieve uniform heating.

2.2 Alloy composition Concerning solid volume fraction and crystal structure, Al-Ge32 is very similar to Al-Si7 (wt.%), an alloy which is commonly used for SSC. Similar to the system Al-Si, Al-Ge features a simple eutectic phase diagram with two two-phase regions in the solid. Because the x-ray absorption contrast in Al-Si7 between the 2 phases is very poor (Al and Si are neighbouring elements), the most convenient way is to replace it by Al-Ge32. That in turn is known to yield very favourable x-ray absorption contrast due to the well separated atomic masses of Al and Ge, allowing one to distinguish between the dense liquid (appearing dark in the radiographs) and the less dense solid particles (characterized by bright contrast) – cf. e.g. [2]. For the injection process, however, one has to expect increased gravitational forces for the germanium-rich liquid phase as well as a lift for the aluminium-rich solid particles, compared to Al-Si.

2.3 Micro-radioscopy The micro-radioscopy experiments were performed on the ID19 beamline of the ESRF. The beamline provides a highly brilliant x-ray beam with the experimental station situated 145 m downstream the light source. In order to achieve a photon flux density high enough to perform fast micro-radioscopy, ID19's white beam mode was chosen. Here, the softer part of the x-ray spectrum is suppressed by a 1 mm thick aluminium absorber. A dedicated detector for synchrotron white beam imaging consisting of an optical system combined with a

Copyright line will be provided by the publisher

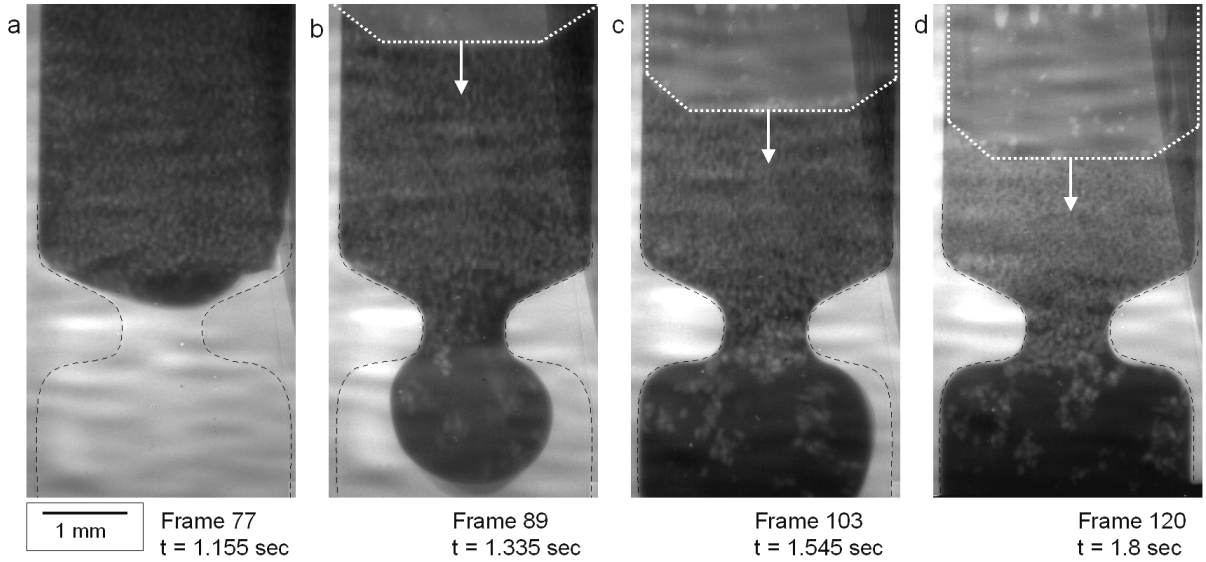

Figure 2 Selected radioscopic images taken at (a) t = 1.155 s, (b) t = 1.335 s, (c) t = 1.545 s and (c) t = 1.8 s after starting the injection. Note that the aluminium-rich solid appears brighter, compared to the germanium-rich liquid which is shown in black.

CMOS camera (PCO.1200 hs, 1280 x 1024 pixels, 10 bit dynamic range (60 dB), 12 µm pixel pitch, up to 1 Gb/s recording speed - PCO AG, Kehlheim, Germany) for fast data acquisition was used [14]. X-ray images were collected at 67 frames/ sec with an effective pixel size of 9 µm. After heating the mould and the alloy to 450°C, the injection was performed by driving a ceramic piston into the mould, thus pushing the semi-solid slurry through the bottleneck. The piston was driven at a speed of v = 2 mm/s using a Newport linear stepping motor. Image acquisition started one second prior to the injection. Since the readout time of the CMOS camera is negligibly short, each frame corresponds to an exposure of 15 ms.

3 Results

Fig. 2 shows four selected radiographic images which illustrate the injection process. These 4 images were taken at t = 1.155 s, 1.335 s, 1.545 s and 1.8 s after the beginning of the measurement [*here could be a link to the video file*]. The liquid phase which appears dark in the radiograph due to its higher x-ray absorption first pours into the bottleneck channel then the recipient while the piston is driven further down (marked by the white dotted line and the arrows in Fig. 2 b-d), first forming a bulb shape due to reduction of its surface tension. The solid phase descends at a much slower pace and only few solid particle clusters detach and are transported along with the liquid into the recipient (see Fig. 2b). Once the bottleneck is filled with slurry, the solid phase can no longer enter the recipient. Some of the few particle clusters which have passed through the channel eventually float up to re-agglomerate with the bulk (the term bulk refers to the continuous network of solid particles above the bottleneck). As a consequence the remaining feedstock material is compressed and the liquid is squeezed through the open-porous solid by the piston (Fig. 2d). An attempt to quantify the two-dimensional flow field by box-wise cross-correlation between consecutive images is shown in Fig. 3. As can be seen, quantitative evaluation of the flow field remains limited to particles which are moving at a speed <1 mm/s. Thus only the downward motion of the bulk material in the reservoir is analysed. Particles and clusters which are moving faster (e.g. when being transported through the bottleneck into the recipient) are obscured by motion-blurring effects.

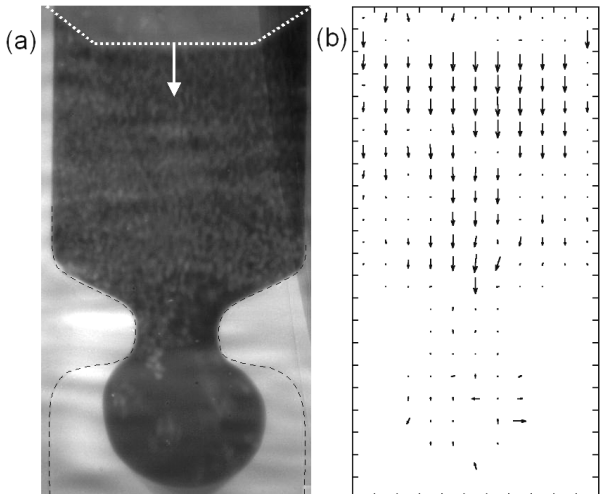

Figure 3 (a) Radiograph corresponding to frame no. 89. (b) Vector representation of the optical flow between two consecutive images (frame 89 and 90) calculated by box-wise cross correlation (box size 32 x 32 pixel).

A short sequence of the early injection is depicted in Fig. 4 in time-steps of 30 ms (2 frames). One can observe how several clusters of solid particles detach from the bulk and are transported into the recipient along the direction of

Copyright line will be provided by the publisher

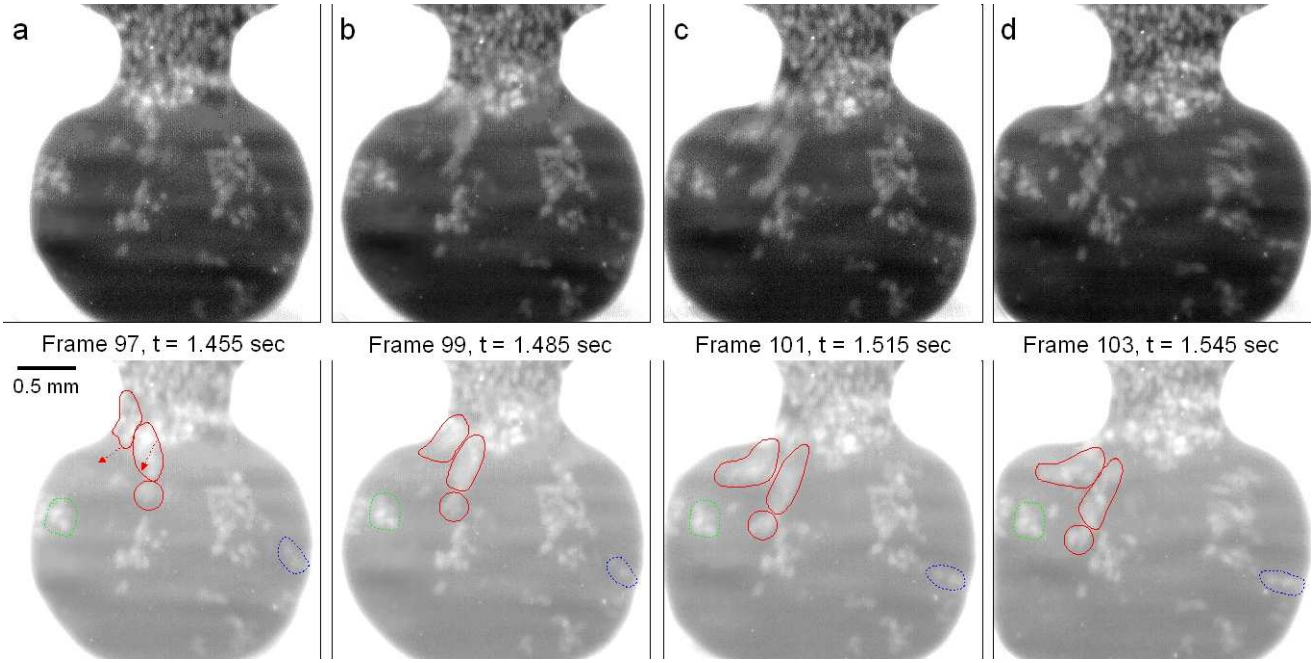

Figure 4 Selected radioscopic images taken at intervals of 30 ms. (a-d) show high velocity transport of small particle clusters into the recipient. Because the fast motion of the particles is obscured by motion blurring estimated particle silhouettes are drawn below.

the fluid flow. The particle motion is blurred due to the fact that these clusters move with a speed significantly higher than 0.6 mm/s – which would be the highest speed captured without motion-blurring. Schematic drawings of some moving particle clusters are illustrated below the radiographs in Fig. 4. From these results we can estimate a maximum particle speed of approx. 6-8 mm/s. This high speed is the result of an accelerated flow of the liquid due to the reduced cross section of the bottleneck. From Fig. 3 we can estimate the liquid speed in the recipient to approx. 5-6 mm/s, consequently the liquid can flow 6 times faster through the channel according to Bernoulli's principle. Our findings are schematized in Fig. 5.

4 Discussion and outlook

The result of this injection process illustrates a well known problem in SSC: a complete filling of the mould is achieved, but a very inhomogeneous microstructure is created as can be seen from Fig. 2d as well as from Fig. 6 showing a metallographic section that was prepared after a similar injection and air cooling. The general conclusion which can be drawn from our results is that semi-solid casting through narrow channels requires de-agglomeration of solid grains and/ or particle clusters to reduce their effective cross-section. The break-off of such clusters shows a need for high velocities in the surrounding fluid which is why de-agglomeration is mainly observed in or just below the bottleneck cavity where the fluid flow reaches a maximum speed. Once a cluster has detached from the bulk it accelerated to a speed which is – for a short time - comparable to that of the fluid flow. Soon after de-agglomeration the particle clusters tend to re-agglomerate and flow upwards due to their density which is lower than the fluids'. Thus, the filling remains anisotropic: The concentration of aluminium in the recipient is much lower compared to the reservoir, due to the lower viscosity of the Al-poor liquid which penetrated the cavity more easily. The apparently strong mutual attraction of the detached solid grains remains to be further examined both experimentally and in theory including possible long-range interactions between particles via concentration gradients in the liquid.

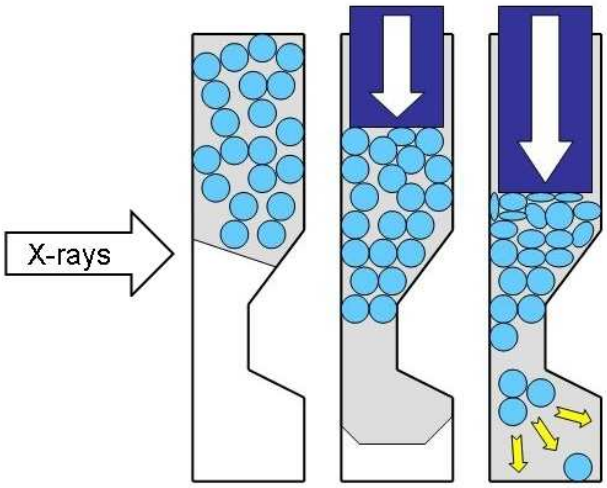

Figure 5 Schematic side view showing the injection.

With this work we have successfully demonstrated that in situ imaging of semi-solid flow is possible with fast synchrotron-based micro-radioscopy. The solid aluminium-rich particles can be clearly distinguished from the Al-Ge melt. Qualitatively we observed de- and re-agglomeration of solid particle clusters which are in accor-

Copyright line will be provided by the publisher

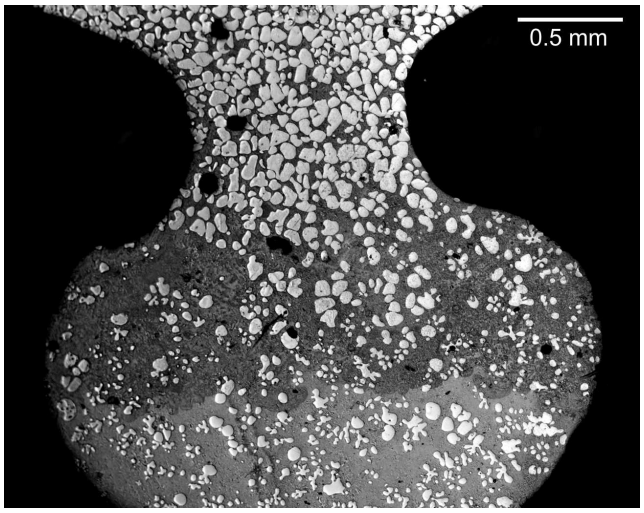

Figure 6 Metallographic section of the Al-Ge32 material prepared after a similiar injection experiment.

dance with theory for semi-solid flow of metal alloys [15]. Obviously quantitative analysis of both the liquid flow and the high solid cluster velocities (e.g. in the bottleneck cavity) require higher frame rates. Hence, the main goal for further experiments is to achieve better temporal resolution. Concerning our experiment, we plan several steps to improve the performance in terms of contrast and acquisition speed. Performing the experiment at beamlines where the experiment is closer to the source and the x-ray beam is less divergent, one would obtain at least 1-2 orders of magnitude more photon flux thus enabling radioscopy at 500 frames/ sec and faster. Observations of pore-coalescence in liquid metal foam were already reported with an acquisition rate of 40 000 frames/ sec on the ID15A beamline of the ESRF [16]. In addition to the high-speed the advantages of in-situ radiography compared to conventional metallographic sectioning are rather obvious (see Fig. 6). Polished sections only show a part of the structure and do not contain "in depth" information. Hence, the obvious de- and re-agglomeration of larger particle clusters can only be tracked by radioscopy (Fig. 4), not in visible light microscopy (Fig. 6, note that there is a second crystallization during cooling since the experiment is carried out ca. 30 °C above the solidus temperature). Despite being very fast, radioscopy data represents only an average intensity, summing the x-ray attenuation of all material along the beam. Consequently such experiments will always be limited to comparatively thin cavities (with respect to the average particle diameter) in order to avoid superposition of many particles.

Concerning the image analysis, optical flow methods might allow us to extract more quantitative information from the radioscopic sequences once a higher frame rate is achieved [17,18]. With the potential of our method we believe that new insights into flow processes during SSC can be obtained.

Acknowledgements The authors acknowledge T. Martin and J.P. Valade (ESRF) for technical support during the experiments. Our gratitude further goes to M. Klinger and H. Heimbach (BAM Berlin, Germany) for construction. C. Leistner, C. Förster (Helmholtz-Centre Berlin, Germany) as well as T. Baumbach (ANKA Karlsruhe, Germany) and J. Baruchel (ESRF Grenoble, France) are thanked for their assistance and generous help.

References

[1] M. C. Flemings 1991 *Metall. Trans. A* **22A** 957–81.
[2] S. Zabler, A. Rueda, A. Rack, H. Riesemeier, P. Zaslansky, I. Manke, F. Garcia-Moreno and J. Banhart 2007 *Acta Mater.* **55** 5045–55.
[3] G. Reinhart, A. Buffet, H. Nguyen-Thi, B. Billia, H. Jung, N. Mangelinck-Noel, N. Bergeon, T. Schenk, J. Hartwig and J. Baruchel 2008 *Metall. Trans. A* **39A** 865–74.
[4] A. King, G. Johnson, D. Engelberg, W. Ludwig and J. Marrow 2008 *Science* **321** 382–5.
[5] A. K. Dahle and D. H. St.John 1998 *Acta Materialia* **47** 31–41.
[6] Z. Fan 2002 *International Materials Reviews* **47** 49-85.
[7] D. B. Spencer, R. Mehrabian and M. C. Flemings 1972 *Metall. Trans. B* **3** 1925–32.
[8] L. S. Turng and K. K. Wang 1991 *J. Mater. Sci.* **26** 2173–83.
[9] V. Laxmanan and M. C. Flemings 1980 *Metall. Trans. A* **11A** 1927–37.
[10] F. Ilinca, J.-F. Hétu, J.-F. Moisan and F. Ajersch 2008 *Int. J. Mater. Form.* **1** 3–12.
[11] M. Hufschmidt, M. Modigell and J. Petera 2006 *J. Non-Newtonian Fluid Mech.* **134** 16–26.
[12] J. N. Koster, T. Seidel and R. Derebeil 1997 *J. Fluid Mech.* **343** 29–41.
[13] S. Boden, S. Eckert, B. Willers and G. Gerbeth 2008 *Metall. Trans. A* **39A** 613–23.
[14] F. García-Moreno, A. Rack , L. Helfen, T. Baumbach, S. Zabler, N. Babcsán, J. Banhart, T. Martin, C. Ponchut and M. Di Michiel 2008 *Appl. Phys. Lett.* **92** 134104 1 - 3.
[15] M. Perez, J.-C. Barbé, Z. Neda, Y. Bréchet and L. Salvo 2000 *Acta Mater.* **48** 3773–82.
[16] A. Rack, F. García-Moreno, T. Baumbach and J. Banhart 2009 *J. Synchrotron Radiat.* **16** 432–4.
[17] B. Jähne 2005 *Digital Image Processing: Concepts, Algorithms, and Scientific Applications* (Springer).
[18] O. Betz, A. Rack, C. Schmitt, A. Ershov, A. Dieterich, L. Körner, D. Haas and T. Baumbach 2008 *Synchrotron Radiation News* **21** 34–8.

Copyright line will be provided by the publisher